Available online at www.sciencedirect.com

SciVerse ScienceDirect

Procedia Engineering 48 (2012) 436 – 444

Procedia Engineering

www.elsevier.com/locate/procedia

MMaMS 2012

3D beam finite element including nonuniform torsion

Justín Murín[a]*, Vladimír Kutiš[a], Viktor Královič[a], Tibor Sedlár[a]

[a]*Department of Applied Mechanics and Mechatronics of IPAEE, FEI STU in Bratislava, Ilkovčova 3, 812 19 Bratislava, Slovakia*

Abstract

New 3D beam finite element including non-uniform torsion will be presented in this contribution which is suitable for analysis of beam structures of open and closed cross-sections. The secondary torsion moment deformation effect will be included into the stiffness matrix. Results of the numerical experiments will be discussed and evaluated.

Keywords: Non-uniform torsion, 3D beam finite element, secondary torsion moment deformation effect, closed thin walled cross

Nomenclature

u^e	nodal displacement vector
F^e	nodal load vector
u, v, w	displacement (m)
$N, T_{y,z}$	normal and shear forces (N)
M_x, M_T	torsion moment (Nm)
$M_{y,z}$	bending moments (Nm)
M_ω	bimoment (Nm^2)
$k_{i,j}$	stiffness coefficient
I_y, I_z	quadratic area moments of inertia (m^4)
I_T	torsion constant (m^4)
I_ω	warping constant (m^6)
I_{Ts}	secondary torsion constant (m^4)
E	Young's modulus (MPa)
G	shear modulus (MPa)

Greek symbols

ν	Poisson ratio

* Corresponding author. Tel.: 0903251413.
E-mail address: justin.murin@stuba.sk

doi:10.1016/j.proeng.2012.09.537

$\varphi_{x,y,z}$	angular displacement
ϑ'_M	warping part of the twist angle first derivative (m^{-1})
ω	section ordinate (m^2)
σ_ω	normal stress caused by bimoment (MPa)
σ_{Mz}	normal bending stress (MPa)
τ_p	primary shear stress (MPa)
τ_s	primary shear stress (MPa)
Subscripts	
i,j,k	nodal point
R	at corners
an	analytical

1. Introduction

The effect of warping must be assumed in stress and deformation analyses of structures above all with thin-walled cross-sections loaded by torsion. Warping effects occur mainly at the points of action of the concentrated torsion moments (except for free beam ends) and at sections with free-warping restrictions. Special theories of torsion with warping – non-uniform torsion – have been used to solve such problems analytically (e.g. [1]). The analogy between the 2nd order beam theory (with tensional axial force) and torsion with warping is also very often used (e.g. [2], [3]). One has to point out that in the literature and practice, as well as in the EC-3 [4] and EC-9 [5] guidelines, strong warping is assumed to occur in open cross-sections only. Warping-based stresses and deformations in closed sections, however, are assumed to be insignificant and have been therefore neglected.

According to the above mentioned theory of torsion of open cross-sections with warping and the analogy, special 3D-beam finite elements have been designed and implemented into the finite element codes (e.g. [6], [7]). The warping effect is included through an additional degree of freedom at each nodal point - the first derivative of the angle of twisting of the beam cross-section. Important progress in the solution of torsion with warping has been reached in papers [8] and [9] where a combination of boundary and finite element method was used allowing a warping analysis for composite beams with longitudinally varying cross-section.

However, latest theoretical results have shown that the effect of warping must be considered in the case of non-uniform torsion of closed-section beams [10]. For prismatic beams, the analogy between the torsion with warping (including the secondary torsion moment deformation effect) and the 2nd order beam theory (including the shear force deformation effect) has to be used. This approach was implemented into the computer code IQ-100 [13]. This analogy does not hold for non-prismatic beams [11]. According to the last research results in this area ([10], [11], [12], [14]), the local stiffness relation of a new two-node finite element for torsion with warping of straight beam structures is presented in contribution [15]; again based on the above-mentioned analogy. The warping part of the first derivative of the twist angle has been considered as the additional degree of freedom in each node at the element ends which can be regarded as part of the twist angle curvature caused by the warping moment. This new finite element can be used in non-uniform torsion analyses of open and closed cross-section beams. Finally in [16], the boundary element method has been applied in the non-uniform torsion analysis of simply or multiplies connected bars of doubly symmetrical arbitrary constant cross-section, taking into account secondary torsion moment deformation effects. Necessity of the non-uniform torsion effect in the analysis of close shaped cross-section has been confirmed.

In this paper, a new 3D beam finite element will be presented which is suitable for structural analysis of 3D beam structures. The classic 12x12 local stiffness matrix of the 3D beam finite element will be enhanced to 14x14 stiffness matrix. The warping part of the first derivative of the twist angle has been considered as the additional degree of freedom in each node at the element ends which can be regarded as part of the twist angle curvature caused by the warping moment. The transformation of the local finite element equation to the global finite element equation will be done. The derived finite element equations will be implemented into the computer program and the numerical experiments will be done. Results of the numerical analysis concerning the spatial combined loading of chosen beam structures of open and closed cross-section will be presented and discussed.

2. The local and global finite element equations

2.1. Local finite element equation

Figure 1 shows a prismatic beam element of length L with two nodes i and k, and with appropriated geometric, static, kinematics and material quantities: A [m^2] is the double symmetric cross-sectional area; I_y [m^4] and I_z [m^4] are the quadratic area moments of inertia; I_T [m^4] is the torsion constant; I_ω [m^6] is the warping constant, I_{Ts} [m^4] is the secondary torsion constant; E is the Young's modulus; G is the shear modulus. In order to include the warping, a new degree of freedom is added to the classical nodal variables in the stiffness matrix in each element nodal point. The warping part of the first derivative of the twist angle (ϑ'_M) has been considered as the additional degree of freedom in each node at the element ends [15]. This can be regarded as part of the twist angle curvature which is caused by the warping moment. This choice brings advantages when applying the boundary conditions. If the secondary torsion moment deformation effect is not considered $\vartheta'_M(x) = \vartheta'(x)$.

The nodal displacement vector in the local coordinate system, as shown in Fig. 1, is

$$\left\{u^e\right\}^T = \left\{u_i \quad v_i \quad w_i \quad \varphi_{xi} \quad \varphi_{yi} \quad \varphi_{zi} \quad \vartheta'_{Mi} \quad u_k \quad v_k \quad w_k \quad \varphi_{xk} \quad \varphi_{yk} \quad \varphi_{zk} \quad \vartheta'_{Mk}\right\} \tag{1}$$

and the respective nodal load vector is

$$\left\{F^e\right\}^T = \left\{N_i \quad T_{yi} \quad T_{zi} \quad M_{xi} \quad M_{yi} \quad M_{zi} \quad M_{\omega i} \quad N_k \quad T_{yk} \quad T_{zk} \quad M_{xk} \quad M_{yk} \quad M_{zk} \quad M_{\omega k}\right\} \tag{2}$$

where M_{Ti} and M_{Tk} are the torsion moments, $M_{\omega i}$ and $M_{\omega k}$ are the warping moments at the nodal points. The geometrical meaning of all other kinematics and static variables is evident from Figure 1.

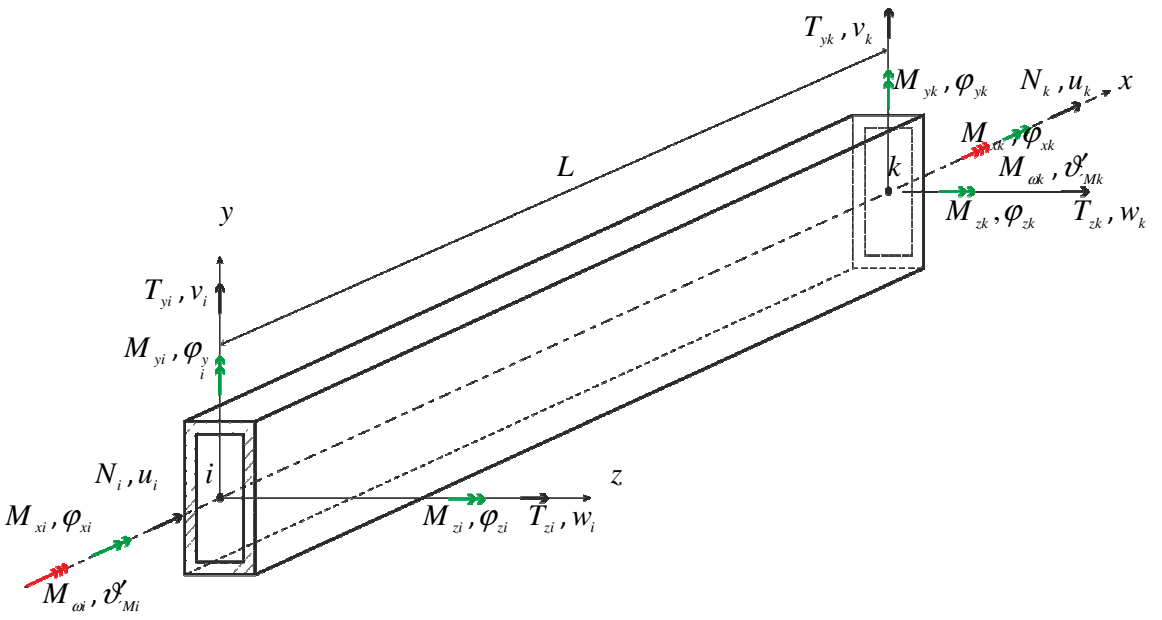

Fig. 1. 3D beam element including non-uniform torsion in local coordinate system.

By enhancing the classic 3D beam finite element about the local stiffness matrix of non-uniform torsion of straight rod [15] we get the local element equation of the 3D beam finite element including the non-uniform torsion with effect of

secondary torsion moment deformation effect:

$$\begin{bmatrix} N_i \\ T_{yi} \\ T_{zi} \\ M_{xi} \\ M_{yi} \\ M_{zi} \\ M_{\omega i} \\ N_k \\ T_{yk} \\ T_{zk} \\ M_{xk} \\ M_{yk} \\ M_{zk} \\ M_{\omega k} \end{bmatrix} = \begin{bmatrix} k_{1,1} & 0 & 0 & 0 & 0 & 0 & 0 & k_{1,8} & 0 & 0 & 0 & 0 & 0 & 0 \\ & k_{2,2} & 0 & 0 & 0 & k_{2,6} & 0 & 0 & k_{2,9} & 0 & 0 & 0 & k_{2,13} & 0 \\ & & k_{3,3} & 0 & k_{3,5} & & 0 & 0 & 0 & k_{3,10} & 0 & k_{3,12} & 0 & 0 \\ & & & k_{4,4} & 0 & 0 & k_{4,7} & 0 & 0 & 0 & k_{4,11} & 0 & 0 & k_{4,14} \\ & & & & k_{5,5} & 0 & 0 & 0 & 0 & k_{5,10} & 0 & k_{5,12} & 0 & 0 \\ & S & & & & k_{6,6} & 0 & 0 & k_{6,9} & 0 & 0 & 0 & k_{6,13} & 0 \\ & & Y & & & & k_{7,7} & 0 & 0 & 0 & k_{7,11} & 0 & 0 & k_{7,14} \\ & & & M & & & & k_{8,8} & 0 & 0 & 0 & 0 & 0 & 0 \\ & & & & M & & & & k_{9,9} & 0 & 0 & 0 & k_{9,13} & 0 \\ & & & & & E & & & & k_{10,10} & 0 & k_{10,12} & 0 & 0 \\ & & & & & & T & & & & k_{11,11} & 0 & 0 & k_{11,14} \\ & & & & & & & R & & & & k_{12,12} & 0 & 0 \\ & & & & & & & & Y & & & & k_{13,13} & 0 \\ & & & & & & & & & & & & & k_{14,14} \end{bmatrix} \cdot \begin{bmatrix} u_i \\ v_i \\ w_i \\ \varphi_{xi} \\ \varphi_{yi} \\ \varphi_{zi} \\ \vartheta'_{Mi} \\ u_k \\ v_k \\ w_k \\ \varphi_{xk} \\ \varphi_{yk} \\ \varphi_{zk} \\ \vartheta'_{Mk} \end{bmatrix} \tag{4}$$

The stiffness terms in (14) are: $k_{1,1} = k_{8,8} = -k_{1,8} = -EA/L$; $k_{2,2} = k_{9,9} = -k_{2,9} = 12EI_z/L^3$; $k_{2,6} = k_{2,13} = 6EI_z/L^2$; $k_{3,3} = k_{10,10} = -k_{3,10} = 12EI_y/L^3$; $k_{3,5} = -k_{3,12} = -k_{10,12} = k_{10,12} = -6EI_y/L^2$; $k_{4,4} = k_{11,11} = -k_{4,11} = ck_1/\kappa k_2$; $k_{4,7} = k_{4,14} = -k_{7,11} = -k_{11,14} = -c = -k_2/\left(\kappa k_2^2 - k_1 k_3\right)$; $k_{5,5} = k_{12,12} = 4EI_y/L$; $k_{6,6} = k_{13,13} = 4EI_z/L$; $k_{7,7} = k_{14,14} = \left(\kappa b_1 - b_0 k_2/k_2\right)$; $k_{7,14} = k_3/k_2$; $k_{6,9} = k_{9,13} = -6EI_z/L^2$; $k_{6,13} = 2EI_z/L$; $k_{5,12} = 2EI_y/L$.

With $K = \kappa \dfrac{GI_T}{EI_\omega}$, $f = \sqrt{K}$ and $x = L$ being the transfer constants b_j calculated as:

$b_0 = \cosh(fx)$, $b_1 = \dfrac{\sinh(fx)}{f}$, for $j \geq 2 : b_j = \dfrac{b_{j-2} - a_{j-2}}{K}$ and with $a_0 = 1$, for $j \geq 1 : a_j = \dfrac{x^j}{j!}$.

The stiffness constants are: $k_1 = \dfrac{b_1}{EI_\omega}$; $k_2 = \dfrac{b_2}{EI_\omega}$; $k_3 = \left(\dfrac{b_3}{EI_\omega} - \dfrac{b_1}{GI_{Ts}}\right)$.

The arbitrary cross-sectional characteristics are described by: A – cross-sectional area [m^2]; I_T – torsion constant [m^4]; I_{Ts} – secondary torsion constant [m^4]; I_ω - warping constant [m^6]. Material properties: E – elasticity modulus; G – shear modulus.

The secondary torsion moment deformation effect is encountered through constant $\kappa = \left(1 + \dfrac{I_T}{I_{Ts}}\right)^{-1}$ and the transfer constants b_j, $j \in \langle 0,3 \rangle$. Parameter $\kappa = 1$ if this effect is neglected. This is usually made in the case of open form cross-sections where the effect of the secondary torsion moment has been assumed insignificant. Deformation effect of the secondary torsion moment must be considered first of all in the case of the closed form cross-sections as demonstrated in [3].

The expressions for calculation of the secondary torsion constant (denoted as I_{Ts}) depend on the cross-section type. These can be found in [8] and [12], for example. When the kinematic and static variables in Eq. (4) are known at the nodal points, the nodal forces, bending moments, primary and secondary torsion moment, normal and shear stress can be calculated in a usual way [19]. The nodal points' secondary torsion moments are:

$$M_{Tsi} = \kappa\left(M_{Ti} - GI_T \vartheta'_{Mi}\right); \; M_{Tsk} = \kappa\left(M_{Tk} - GI_T \vartheta'_{Mk}\right). \tag{5}$$

The primary torsion moments at the nodal points are:

$$M_{Tpi} = M_{Ti} - M_{Tsi};\;\; M_{Tpk} = M_{Tk} - M_{Tsk}\,. \tag{6}$$

Expressions for the shear and normal stress calculation depend on the cross-sectional area type. This problem has been described in detail in [10]. These expressions will be used for stress calculations in our numerical examples.
For the straight beam structures the local relation (4) coincides with the global one. This new finite element can be used for analysis of torsion with warping of constant both open and closed-shaped cross-sections. The implementation of the expression (4) into the local equation of the general 3D-beam finite element is straightforward, and it will be done in the next chapter.

2.2. Global finite element equation

Local element stiffness matrix (4) after formation has to be transformed to global coordinate system. The transformation is performed by extended transformation matrix and can be formally expressed as

$$K_G = T^T K_L T; \tag{7}$$

where K_L is local element stiffness matrix, T is transformation matrix and K_G is element stiffness matrix transformed to global coordinate system. Transformation matrix T has dimension 14x14 and can be expressed as

$$T = \begin{bmatrix} T_a & 0 & 0 & 0 & 0 & 0 \\ 0 & T_a & 0 & 0 & 0 & 0 \\ 0 & 0 & 1 & 0 & 0 & 0 \\ 0 & 0 & 0 & T_a & 0 & 0 \\ 0 & 0 & 0 & 0 & T_a & 0 \\ 0 & 0 & 0 & 0 & 0 & 1 \end{bmatrix}; \tag{8}$$

where submatrix T_a with dimension 3x3 has classical form [ANSYS].

3. Numerical experiments

In this sub-chapter, the authors present a numerical study of a closed-section prismatic beam loaded by non-uniform torsion and a concentrated force (Fig. 8). In the analysis, the bending and non-uniform torsion parameters will be calculated by the new 3D beam finite element. The material properties of the prismatic cantilever aluminium beam (Figure 8) are as follows: Young modulus E = 79 GPa, shear modulus $G = E/(2(1+\nu)) = 31.1$ GPa and Poisson ration $\nu = 0.27$. The applied concentrated force $F^e = 100$ [N] results in beam bending. Restrictions at the clamped end and the application of an concentrated torsion moment $M_T^e = 100$ [Nm] result in non-uniform torsion.

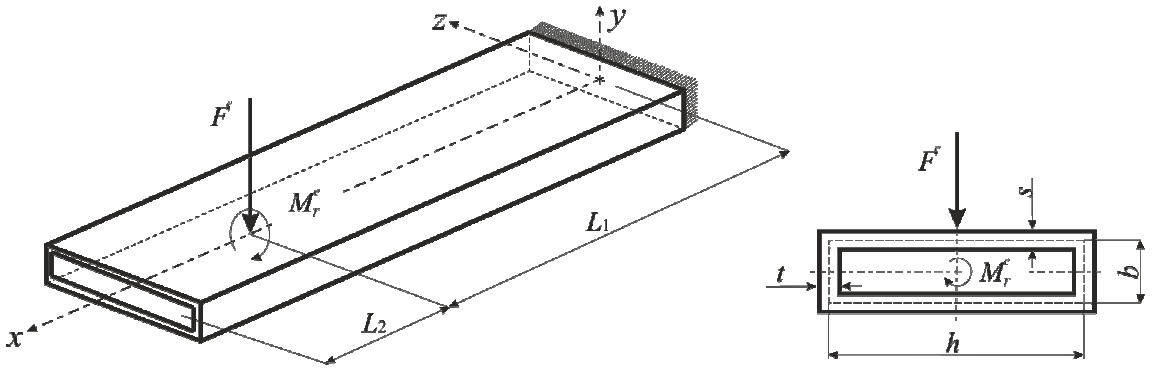

Fig. 2. Geometrical parameters, loads and boundary conditions.

According to Fig. 8, the following geometrical parameters have been chosen and calculated [12], [19]: $L_1 = 0.8$ m, $L_2 = 0.15$ m, $h = 0.058$ m, $b = 0.018$ m, $t = s = 0.002$ m, $A = 2A_s + 2A_G = 2(hs + bt) = 0.000304$ m^2 - the cross-sectional area containing the area of the webs A_s and flanges A_G, warping ordinate at the corners $\omega_R = \frac{hb}{4}\frac{ht - bs}{ht + bs} = 137.368\times10^{-6}$ m^2, warping constant $I_\omega = \omega_R^2 \frac{2A}{3} = 1.91217\times10^{-12}$ m^6, torsion constant $I_T = \frac{2(hb)^2}{h/s + b/t} = 5.73651\times10^{-8}$ m^4, secondary torsion constant $I_{Ts} = \frac{20(h/s + b/t) I_\omega A}{\frac{(Ahb)^2}{A_S A_G} + \frac{2(h^2 + b^2)^2}{3}} = 1.4589\times10^{-8}$ m^4.

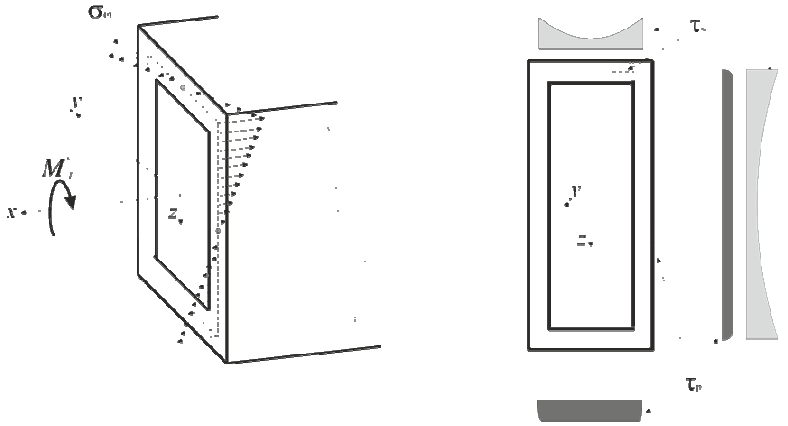

Fig. 3. Normal and shear stress distribution caused by non-uniform torsion. Normal stress caused by bending can be easily calculated using [1].

The authors consider outputs obtained using ANSYS Beam188 and Shell181 elements, the IQ100 software and the new 3D beam element in comparison with the Thin Tube Theory calculations. In the numerical analyses, outputs being the bimoment M_ω, torsion moment M_x, normal stress (from bending σ_{Mz} and bimoment σ_ω), vertical deformation v, bending angle φ_z twist angle φ_x.

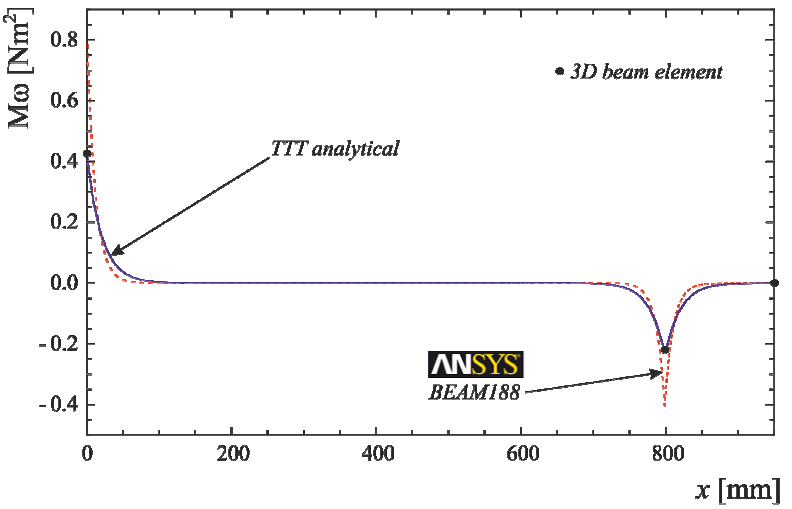

Fig. 4. Bimoment flow as calculated analytically using TTT and numerically via ANSYS Beam188 and via the new 3D beam element.

Bending and warping deformations are calculated separately to point out the advantages of the new 3D beam element in comparison with traditional commercial FEM approach.

Normal and shear stresses (Fig. 9) at any point of the beam can be calculated according to [1], [12], [13] and [18], respectively. For this particular beam and the torsion moment $M_T^e = 100$ Nm, the calculated parameters are as follows: maximal bimoment M_ω = 0.4143 Nm^2, normal stress $\sigma_{\omega,an} = \frac{M_\omega \omega_R}{I_\omega} = \ = 29.77$ MPa, maximal primary shear stress $\tau_{p,\max} = \frac{M_{Tp}}{2hbt} = 23.95$ MPa, maximal secondary shear stress $\tau_{s,\max} = \frac{M_{Ts}}{I_\omega t} \cdot \frac{\omega_R}{\frac{A_G}{4} + \frac{h^2 + b^2}{6(h/s + b/t)}} = 16.27$ MPa. The total torsion angle is $\varphi_x = 2.556^o$.

Table 1: Comparison of obtained analytical and numerical results (nought values are omitted). Please, note the strong miss-calculation in ANSYS Beam188 of non-uniform parameters.

value	unit	TTT	SHELL 181	BEAM 188	3D beam
position 1: x = 0 mm fixed (clamped) support					
F_y	[N]	100	100	100	100
M_z	[Nm]	80	80	79.95	80
σ_{Mz}	[MPa]	34.474	33.211	38.281	34.474
M_x	[Nm]	100	100	100	100
M_ω	[Nm^2]	0.4143	n/a	0.8133	0.4143
σ_ω	[MPa]	34.790	31.993	63.410	29.770
position 2: x = 800 mm load application					
F_y	[N]	100	100	100	100
v	[mm]	-10.07	-10.41	-10.40	-10.34
φ_z	[°]	1.076	1.113	1.111	1.105
M_x	[Nm]	100	100	100	100
φ_x	[°]	2.482	2.567	2.452	2.548
M_ω	[Nm^2]	-0.2072	n/a	-0.3726	-0.2022
σ_ω	[MPa]	-17.395	-15.910	-29.050	-14.530
position 3: x = 950 mm free end					
v	[mm]	-12.90	-13.31	-13.31	-13.25
φ_z	[°]	1.078	1.112	1.111	1.107
φ_x	[°]	2.489	2.571	2.466	2.556

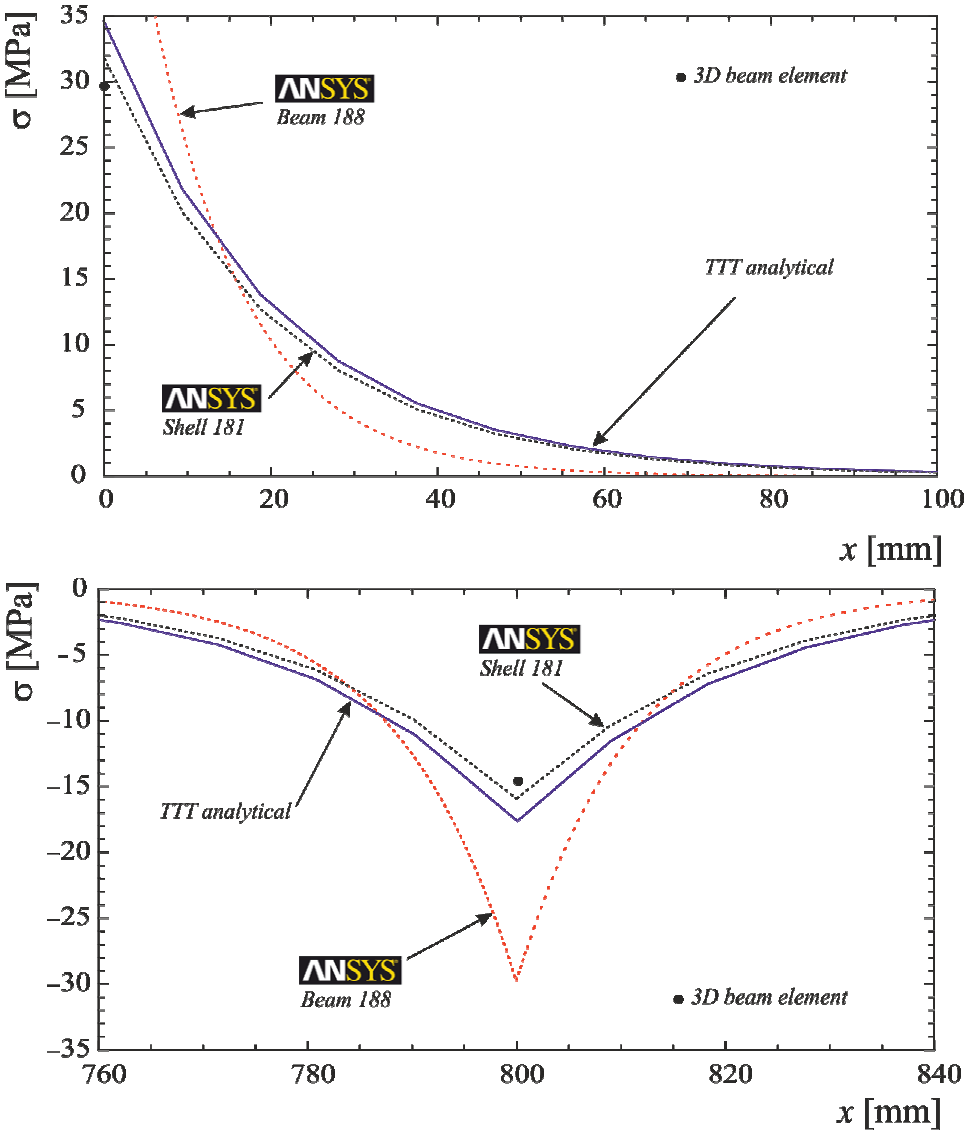

Fig. 5. Maximum normal stress distribution along the beam's longitudinal direction: TTT analytical, ANSYS Beam 188 and Shell 181 element.

In support of the new 3D beam element, the authors wish to point out that using only two new 3D beam elements for this analysis one obtains satisfactory results (see Table 1 and Fig. 11) even for non-uniform torsion parameters. Moreover, the presented results are in very good agreements with the recently obtained experimental data [17].

4. Conclusions

New 3D beam finite element including non-uniform torsion is presented in this contribution which is suitable for analysis of beam structures of open and closed cross-sections. The secondary torsion moment deformation effect has been included into the stiffness matrix. Results of the numerical experiments show very high effectiveness and accuracy of our new beam finite element.

Acknowledgements

This paper has been supported by Grant Agency VEGA (grant No. 1/0534/12).

References

[1] Vlasov, V.Z., 1962. Tenkostěnné pružné prúty, SNTL.

[2] Roik, K., Sedlacek G., 1966. Theorie der Wölbkrafttorsion unter Berücksichtigung der sekundären Schubverformungen - Analogiebetrachtung zur Berechnung des querbelasteten Zugstabes, Stahlbau, 35, p. 43.

[3] Rubin, H., 2005. Wölbkrafttorsion von Durchlaufträgern mit konstantem Querschnitt unter Berücksichtigung sekundärer Schubverformung, Stahlbau, 74, Heft 11, p. 826.

[4] EC-3 Eurocode 3. Design of steel structures.

[5] EC-9 Eurocode 9. Design of aluminium structures.

[6] ANSYS Swanson Analysis System, Inc., 2012. 201 Johnson Road, Houston, PA 15342/1300, USA.

[7] RSTAB, 2006. Ingenieur - Software Dlubal GmbH, Tiefenbach.

[8] Sapountzakis, E.J., Mokos, V.G., 2007. 3-D beam element of composite cross-section including warping and shear deformation effect, Computers and Structures, 85, p. 102.

[9] Mokos, V.G., Sapountzakis, E.J., 2004. 3-D beam element of variable composite cross-section including warping effect, Acta Mechanica, 171 (3-4), p. 703.

[10] Rubin, H., 2007. Torsions-Querschnittswerte für rechteckige Hohlprofile nach EN 10210-2: 2006, Stahlbau, 76, Heft 1.

[11] Rubin, H., 2007. Zur Wölbkrafttorsion geschlossener Querschnitte und ihrer Irrtümer - Grundlagen, 29th Stahlbauseminar, Band 140, ISSN: 1615-4266.

[12] Rubin, H., Aminbaghai, M., 2007. Wölbkrafttorsion bei veränderlichen, offenem Querschnitt - hat die Biegezugstabanalogie noch Gültigkeit?, Stahlbau, 76, p. 747.

[13] Rubin, H., Aminbaghai, M., Weier, H., 2006. IQ-100. The civil engineering structures program, TU Vienna, Bautabellen für Ingenieure, Werner Verlag, 17. Auflage.

[14] Rubin, H., 2007. Baustatik 2, Manuskript der Vorlesung. Institute of Structural Analysis, Vienna University of Technology.

[15] Murin, J., Kutis, V., 2008. An Effective Finite Element for Torsion of Constant Cross-Sections Including Warping with Secondary Torsion Moment Deformation Effect, Engineering Structures, ISSN 0141-0296, Vol. 30, Iss. 10, 2716-2723.

[16] Mokos, V.G., Sapountzakis, E.J., 2011. Secondary torsional moment deformation effect by BEM, International Journal of Mechanical Science. IJMS-10323R1. Accepted for publication.

[17] Murín, J., Sedlár, T., Královič, V., Goga, V., Kalaš, A., Aminbaghai, M., 2012. Numerical Analysis and Measurement of Non-uniform Torsion. Proceedings of the Eleventh International Conference on Computational Structures Technology. Accepted for publication.